



## Methylene blue adsorption onto granular activated carbon prepared from Harmal seeds residue

Maryam Ahmadzadeh Tofighy<sup>a</sup>, Toraj Mohammadi<sup>b,\*</sup>

<sup>a</sup>Department of Chemical Industries, Shahre-Ray Branch, Islamic Azad University, Tehran, Iran

<sup>b</sup>Department of Chemical Engineering, South Tehran Branch, Islamic Azad University, P.O. Box 11365-4435, Tehran, Iran

Tel. +98 21 77240496; Fax: +98 21 77240495; email: torajmohammadi@iust.ac.ir

Received 10 January 2012; Accepted 9 April 2013

---

### ABSTRACT

In this research, application of granular activated carbon prepared from Harmal seeds residue as a new adsorbent for methylene blue (MB) removal from aqueous solutions was investigated. Adsorption equilibrium and kinetic data were studied. The results demonstrated that the equilibrium data were well represented by Langmuir isotherm model, with maximum monolayer adsorption capacity of 1111.11 mg/g. The dimensionless factor ( $R_L$ ) revealed the favorable nature of this adsorption system. The kinetic data were found to follow the pseudo-second-order kinetic model. Effect of initial concentration on the adsorption mechanism of MB onto the prepared activated carbon was also investigated.

*Keywords:* Adsorption; Activated carbon; Methylene blue; Harmal seeds residue; Isotherm; Kinetic

---

### 1. Introduction

Many industries, such as textile, paper, and plastics, use dye in order to color their products and also consume substantial amounts of water. As a result, they generate considerable amounts of colored wastewater. It is recognized that public perception of water quality is greatly influenced by its color. Color is the first contaminant to be recognized in wastewater. The presence of very small amounts of dyes in water (less than 1 ppm for some dyes) is highly visible and undesirable [1–3]. Since dyes have synthetic origins and complex aromatic molecular structures, are inert and difficult to biodegrade when discharged into waste streams. Wastewater containing dyes is very difficult

to treat because dyes are resistant to environmental conditions such as light, heat, and oxidizing agents. From an environmental point of view, removal of synthetic dyes is of great concern, since some dyes and their degraded products may be carcinogenic and toxic and, consequently, their treatment cannot depend on biodegradation alone. This aspect has always been overlooked in their discharge [4].

Methylene blue (MB) as a cationic dye is the most commonly used substance for dyeing cotton, leather, plastics, paper, wood, and silk, as well as for the production of ink and copying paper in the office supplies industry. The chemical structure of MB ( $C_{16}H_{18}N_3SCl$ ) is shown in Fig. 1. MB is a moderate size organic molecule with ionic formula weight of 319 g/mol, cross-sectional area of  $120 \text{ \AA}^2$ , and molecular size of

---

\*Corresponding author.

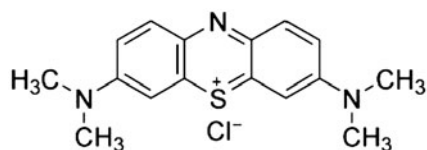


Fig. 1. Chemical structure of MB.

13–15 Å. MB can cause eye burns which may be responsible for permanent injury to the eyes of human and animals [5]. On inhalation, it can give rise to short period of rapid or difficult breathing, while ingestion through mouth produces a burning sensation and may cause nausea, vomiting, profuse sweating, mental confusion, and methemoglobinemia. Acute exposure to MB can cause increased heart rate, vomiting, shock, cyanosis, jaundice, quadriplegia, and tissue necrosis in human [4,6]. Therefore, treatment of effluents containing such dye becomes environmentally important due to its harmful impacts on receiving water.

During the past decades, several physical, chemical, and biochemical decolorization methods have been reported. Among the numerous techniques of dye removal, adsorption gives the best results as it can be used to remove different types of coloring materials [7–9].

Most commercial systems currently use activated carbon as sorbent to remove dyes from wastewater because of its excellent adsorption ability. However, commercially available activated carbons are still considered as expensive materials in many countries due to the use of nonrenewable and relatively expensive starting materials such as coal, which is unjustified in pollution control applications. Therefore, in recent years, a growing research interest has been prompted in production of activated carbons from renewable and cheaper precursors [10–16]. If the raw material is

hard enough, hard particles, granular activated carbon can be obtained that has good resistance and is not easily broken or crushed during oxidation, washing, and drying and also can be used in continuous adsorption processes. Granular activated carbon is used as column filler for gas or liquid applications and is regenerated after use. This makes granular activated carbon a more versatile and expensive adsorbents [17–19].

Harmal (*Peganum harmala*) is a perennial plant that has various medical applications. Harmal is used as an analgesic and antiinflammatory agent. In Yemen, it is used to treat depression. Harmal is a central nervous system stimulant and a “reversible inhibitor of MAO-A (RIMA),” a category of antidepressant. Harmal has “antibacterial activity,” including antibacterial activity against drug-resistant bacteria. Its round seed capsules have three chambers and carry more than 50 seeds (Fig. 2). When its dried capsules or seeds (known in Persian as Esphand) are heated over red hot charcoal or gas flame, they explode with a little popping noise and release a fragrant smoke. The released smoke kills algae, drug-resistant bacteria, intestinal parasites, and molds [20–25].

Harmal seeds is commonly used in many countries and a large amount of its residue is produced which can be considered as a potential cheap precursor for making activated carbon. Harmal seeds residue is a household waste available in huge amount in Iran and many other countries.

This study focused on preparation of Harmal seeds residue-based activated carbon and evaluation of its adsorption potential for MB removal from aqueous solutions. The adsorption equilibrium and kinetic data were then studied to understand the adsorption mechanism of MB molecules onto the prepared activated carbon.

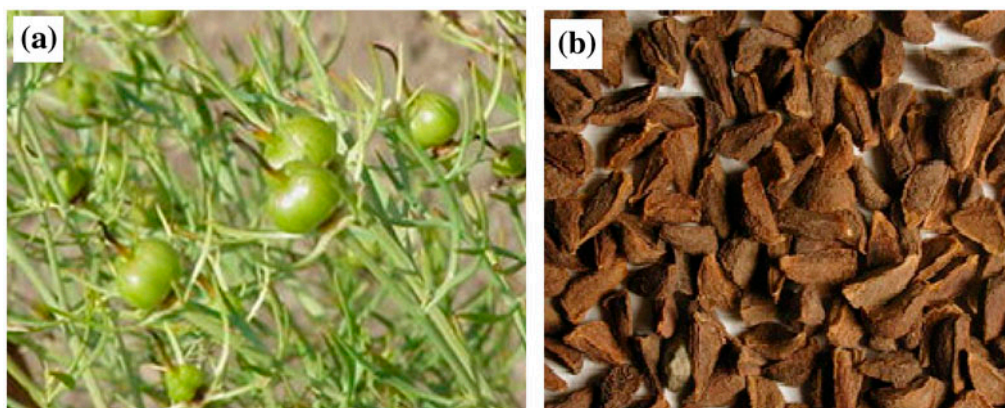


Fig. 2. (a) Harmal seed capsules and (b) Harmal seeds [21].

## 2. Experimental

### 2.1. Materials

The Harmal seeds residue used in this investigation was collected from household. Concentrated nitric acid (HNO<sub>3</sub>; 65%, Merck) was used in activation procedure (acid treatment). MB and distilled water were used to prepare all the solutions.

### 2.2. Adsorbent preparation

As mentioned before, when Harmal seeds are heated, they explode with a little popping noise and release a fragrant smoke. Black materials discarded after using is called Harmal seeds residue. The Harmal seeds residue used in this investigation was collected from household. Two grams of the Hamal seeds residue were soaked in 100 ml of concentrated nitric acid, for 48 h at room temperature. The treated residue was washed using deionized water several times, then dried at 105°C for 24 h, and stored in bottle for use, without crushing.

### 2.3. Characterization of prepared activated carbon

Scanning electron microscope (SEM, Philips: XL30) was used for analysis of the surface morphology of the prepared activated carbon and to verify the presence of porosity. X-ray diffraction analysis (XRD, Philips: 1480) was conducted to investigate the chemical structural of the prepared activated carbon. The chemical compositions of the prepared activated carbon were obtained using elemental analysis (Analyzer, Skalar). Surface functional groups of the Harmal seeds residue and prepared activated carbon were determined by Fourier transform infrared spectroscopy (FTIR, Spectrum: RX1).

### 2.4. Batch adsorption studies

Batch adsorption experiments were carried out by adding 60 mg of prepared activated carbon with granular shape into 50 ml of MB solution at different initial MB concentrations (200, 400, 800, 1,600, and 3,200 ppm). All the experiments were carried out at 25°C and initial pH of about 7. UV–visible spectrophotometer (UV/VIS, Metertech: SP8001) was employed to determine MB concentration, at a wavelength of 670 nm. Each experiment was duplicated under identical conditions. The amount of adsorption at equilibrium,  $q_e$  (mg/g), was calculated by the following equation:

$$q_e = \frac{(C_0 - C_e)V}{w} \quad (1)$$

where  $C_0$  is the initial MB concentration (mg/l),  $C_e$  is the equilibrium MB concentration (mg/l),  $V$  is the volume of MB solution (l), and  $w$  is the mass of dry adsorbent used (g).

### 2.5. Batch kinetics studies

Procedure of kinetics experiments was identical to that of adsorption experiments. The aqueous samples were taken at preset time intervals and MB concentration was similarly measured. The adsorption amount at time ( $t$ ),  $q_t$  (mg/g), was calculated using the following equation:

$$q_t = \frac{(C_0 - C_t)V}{w} \quad (2)$$

where  $C_0$  is the initial MB concentration (mg/l),  $C_t$  (mg/l) is the MB concentration at time  $t$ ,  $V$  is the volume of MB solution (l), and  $w$  is the mass of dry adsorbent used (g).

## 3. Results and discussion

### 3.1. Characterization of Harmal seeds residue-based activated carbon

As mentioned before, the Harmal seeds residue-based activated carbon has granular shape with dimensions of about (2 mm × 2 mm × 3 mm). They have relatively high resistance and are not easily crushed during oxidation, washing, drying, and also adsorption processes. Hence, using the Harmal seeds residue-based activated carbon with granular shape as adsorbent, the problem of carbon removing from water after adsorption process (by centrifuging) is eliminated.

SEM is widely used to study morphological features and surface characteristics of the adsorbent materials. Fig. 3 shows the surface SEM images of the Harmal seeds residue-based activated carbon. As can be observed, many pores with honey comb structure are clearly found on the surface and inside of the prepared activated carbon. The developed pores led to high surface area and porous structure of the Harmal seeds residue-based activated carbon.

A typical XRD pattern of the Harmal seeds residue-based activated carbon is shown in Fig. 4, where there are only two broad small diffraction peaks at around at 23.5° and 43°, which are attributed to the presence of carbon [26,27]. Also, there are not certain

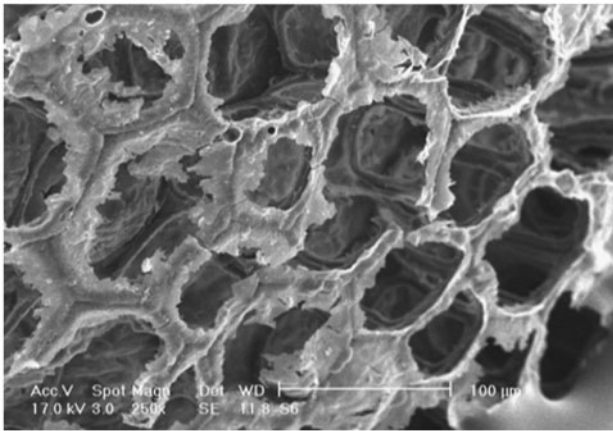


Fig. 3. Surface SEM image of the Harmal seeds residue-based activated carbon.

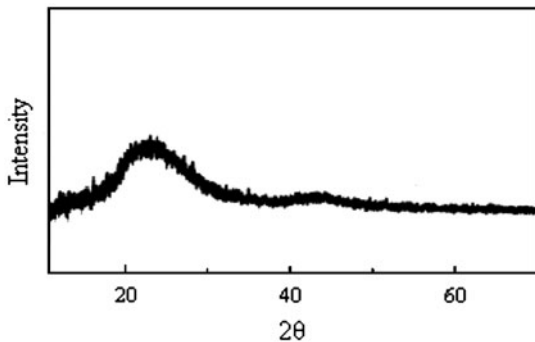


Fig. 4. XRD pattern of the Harmal seeds residue-based activated carbon.

sharp peaks in the XRD pattern, suggesting that the prepared activated carbon exists as amorphous material without any ash. As reported in the literature, the existence of sharp peaks in the XRD pattern can be attributed to the existence of residual ash in carbon [28]. Acid treatment (with  $\text{HNO}_3$ ) can remove inorganic components in carbon such as ash containing K, Ca, Fe, S, ... resulting in higher surface area and pore volume [29,30].

The results of the elemental analysis of the Harmal seeds residue-based activated carbon showed that the prepared activated carbon contains mainly carbon (73%) and oxygen (22%) with small amounts of hydrogen and nitrogen.

Fig. 5 displays the FTIR spectra of Harmal seeds residue and Harmal seeds residue-based activated carbon. As can be observed, the FTIR spectrum of Harmal seeds residue-based activated carbon displays some apparent peaks after acid treatment, indicating formation of oxygen-containing functional groups onto the surface of Harmal seeds residue-based

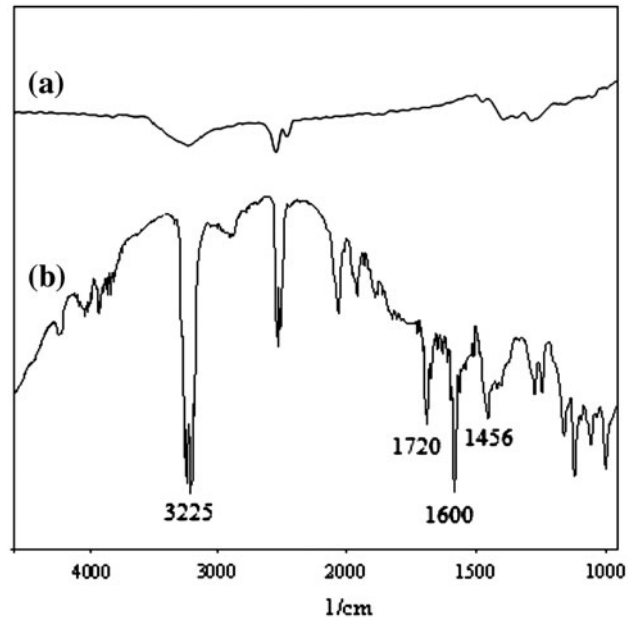


Fig. 5. FTIR spectra of (a) Harmal seeds residue and (b) Harmal seeds residue-based activated carbon.

activated carbon: hydroxyl groups ( $-\text{OH}$ ) ( $3,225\text{ cm}^{-1}$ ), carboxyl groups ( $-\text{COOH}$ ) ( $1,600\text{ cm}^{-1}$ ), and carbonyl groups ( $\text{C}=\text{O}$ ) ( $1,456\text{ cm}^{-1}$ ) [31]. The characteristic peaks at approximately  $1,720$  and  $3,225\text{ cm}^{-1}$  are attributed to the  $\text{C}=\text{O}$  and  $\text{O}-\text{H}$  bonds which indicate formation of the carboxyl groups ( $-\text{COOH}$ ) on the surface of prepared activated carbon. The increased intensity of the peak at  $3,225\text{ cm}^{-1}$  after acid treatment indicates formation of the hydroxyl groups ( $-\text{OH}$ ) on the surface of prepared activated carbon [32–36]. These functionalized groups can provide a large number of chemical adsorption sites and thereby can increase the adsorption capacity of prepared activated carbon [37–42]. Meanwhile, the hydrophilic properties of these functional groups improve the dispersivity of prepared activated carbon in aqueous solutions [42].

### 3.2. Effect of contact time and initial MB concentration on adsorption equilibrium

Fig. 6 shows effect of contact time on adsorption capacity at various initial MB concentrations at  $25^\circ\text{C}$ . The amount of MB adsorbed onto the prepared activated carbon increases with time and then reaches to equilibrium. Also, the equilibrium time increases significantly with increasing initial MB concentration. Obviously, at higher initial MB concentrations, effect of the concentration boundary layer is more significant, and consequently, longer time is needed to attain equilibrium due to the more MB molecules. As shown in Fig. 6, the contact time needed for the MB solutions

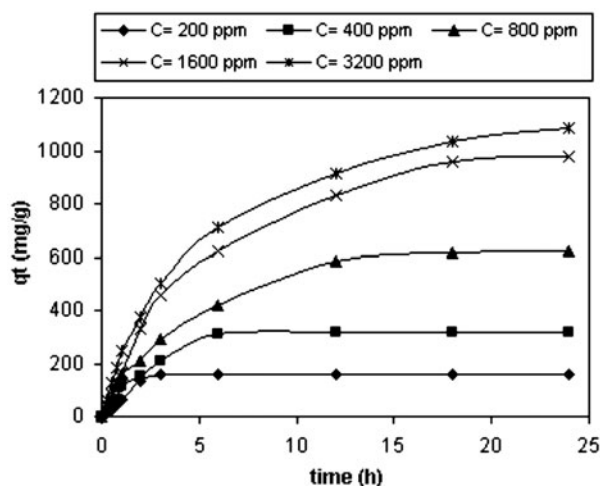


Fig. 6. Effect of initial MB concentrations on adsorption capacity of MB onto the Harmal seeds residue-based activated carbon.

to reach in equilibrium at various initial MB concentrations is within 2–24 h for the Harmal seeds residue-based activated carbon.

The amount of MB adsorbed at equilibrium reflects the maximum adsorption capacity ( $q_e$ ) of the adsorbent under those operating conditions. In Fig. 6, it can be observed that with increasing initial MB concentration from 200 to 3,200 ppm, the adsorption capacity increases from 158 to 1,083 mg/g. It can be said that, at higher initial MB concentration, the mass transfer driving force becomes larger, and hence resulting in more adsorption of MB molecules [5,43].

### 3.3. Adsorption isotherms

Equilibrium adsorption isotherm is basically important to describe how solutes interact with adsorbents, and is critical in optimizing the use of adsorbents [44]. Fig. 7 shows equilibrium adsorption isotherm of MB onto the Harmal seeds residue-based activated carbon.

Adsorption isotherm study was carried out using Langmuir and Freundlich isotherm models.

Langmuir isotherm was used successfully to characterize the monolayer adsorption process [45]. The Langmuir isotherm is given by the following equation:

$$\frac{C_e}{q_e} = \frac{1}{Q_0 b} + \frac{1}{Q_0} C_e \quad (3)$$

where  $C_e$  is the equilibrium adsorbate concentration (mg/l),  $q_e$  is the amount of adsorbate adsorbed per unit mass of adsorbent (mg/g), and  $Q_0$  and  $b$  are the

Langmuir constants related to adsorption capacity and adsorption rate, respectively. When  $C_e/q_e$  is plotted against  $C_e$ , a straight line with slope of  $1/Q_0$  is obtained (Fig. 8(a)). The Langmuir constants (calculated using Eq. (3)) are listed in Table 1.

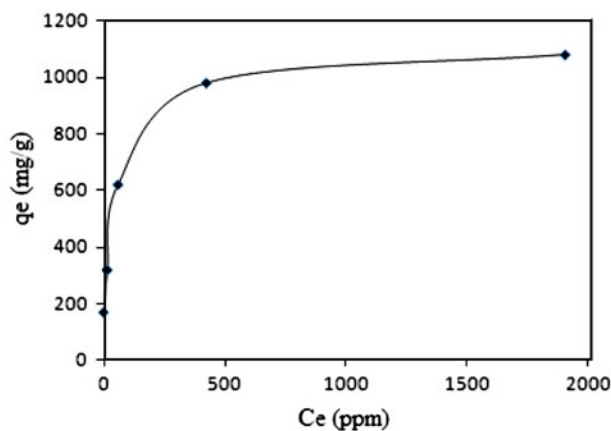


Fig. 7. Equilibrium adsorption isotherm for adsorption of MB onto the Harmal seeds residue-based activated carbon.

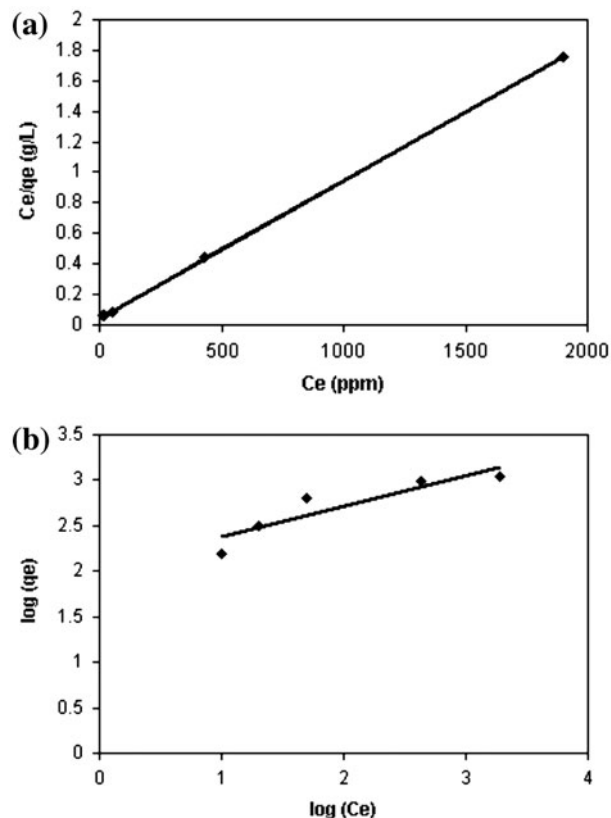


Fig. 8. (a) Langmuir and (b) Freundlich adsorption isotherms for adsorption of MB onto the Harmal seeds residue-based activated carbon.

Table 1

Langmuir and Freundlich isotherm model parameters and correlation coefficients for adsorption of MB onto the Harmal seeds residue-based activated carbon

Models	Langmuir				Freundlich		
	$Q_0$ (mg/g)	$b$ (L/mg)	$R_L$	$R^2$	$K_F$	$1/n$	$R^2$
	1111.11	0.02	0.02	0.99	107.99	0.34	0.84

The essential characteristics of Langmuir isotherm can be expressed in terms of a dimensionless equilibrium parameter ( $R_L$ ) [45]. This parameter is defined as:

$$R_L = \frac{1}{1 + bC_0} \quad (4)$$

where  $b$  is the Langmuir constant and  $C_0$  is the highest initial MB concentration (mg/l). The value of  $R_L$  indicates the type of the isotherm to be either unfavorable ( $R_L > 1$ ), linear ( $R_L = 1$ ), favorable ( $0 < R_L < 1$ ) or irreversible ( $R_L = 0$ ).

Freundlich isotherm is a semi-empirical equation based on adsorption occurred on heterogeneous surfaces [45]. The well-known logarithmic form of Freundlich isotherm is given by the following equation:

$$\log q_e = \log K_F + \left(\frac{1}{n}\right) \log C_e \quad (5)$$

where  $C_e$  is the equilibrium adsorbate concentration (mg/l),  $q_e$  is the amount of adsorbate adsorbed per unit mass of adsorbent (mg/g), and  $K_F$  and  $n$  are the Freundlich constants related to adsorption capacity and adsorption rate, respectively. Plot of  $\log q_e$  vs.  $\log C_e$  gave straight line with slope of  $1/n$ , as shown in Fig. 8(b). Accordingly, the Freundlich constants (calculated using Eq. (5)) are listed in Table 1.

Table 1 summarizes all the constants and correlation coefficients of Langmuir and Freundlich isotherm models. Applicability of the isotherm models to describe the adsorption process was judged by the correlation coefficient ( $R^2$ ) values. As observed in Table 1, Langmuir model agrees well with the experimental data, with the correlation coefficient values being close to one, as compared with Freundlich model. Also, the obtained  $R_L$  values indicate that Langmuir isotherm model is favorable for adsorption of MB onto the Harmal seeds residue-based activated carbon. Conformation of the experimental data with Langmuir isotherm equation indicates the homogeneous nature of Harmal seeds residue-based activated

carbon surface, i.e. each MB molecule/Harmal seeds residue-based activated carbon has equal adsorption activation energy. Similar observation was reported by Tan et al. [44] and Hameed et al. [4]. The results also demonstrated formation of monolayer coverage of MB molecules to the outer surface of prepared activated carbon with maximum monolayer adsorption capacity of 1111.11 mg/g.

Since the adsorption process of MB was well described by Langmuir isotherm model, the maximum monolayer adsorption capacity (for complete monolayer coverage) could be used to evaluate the available surface area of the prepared activated carbon [46]. The following formula was used to compute this surface area ( $S$ ,  $m^2/g$ ):

$$S = \frac{N_A \times A_m \times Q_0}{M_W \times 1000} \quad (6)$$

where  $Q_0$  is the maximum monolayer adsorption capacity (mg/g),  $N_A$  is the Avogadro's number,  $M_W$  is the molecular weight of MB (319.86 g/mol), and  $A_m$  is the area occupied by an adsorbed MB molecule ( $120 \text{ \AA}^2$ ). The calculated surface area of the prepared activated carbon is  $2510.68 \text{ m}^2/g$ . For comparison, the range of surface area in commercial activated carbons is  $2,000\text{--}5,000 \text{ m}^2/g$ .

### 3.4. Adsorption kinetics

In order to analyze the adsorption mechanism of MB molecules onto the Harmal seeds residue-based activated carbon, three kinetic models including the pseudo-first-order, the pseudo-second-order, and the intraparticle diffusion models were applied to fit the experimental data under different initial MB concentrations.

The rate constant of adsorption can be determined using the pseudo-first-order equation given by Lagergren and Svenska [47] as:

$$\ln(q_e - q_t) = \ln q_e - \frac{k_1}{2.303} t \quad (7)$$

where  $q_e$  and  $q_t$  are the amounts of adsorbate adsorbed per unit mass of adsorbent (mg/g) at equilibrium and at time  $t$  (min), respectively, and  $k_1$  ( $\text{min}^{-1}$ ) is the rate constant of first-order adsorption.

The pseudo-second-order equation [48] based on equilibrium adsorption can be expressed as:

$$\frac{t}{q_t} = \frac{1}{k_2 q_e^2} + \frac{1}{q_e} t \quad (8)$$

where  $k_2$  (g/mgmin) is the rate constant of the second-order adsorption.

The slope and the intercept of each linear plot in Fig. 9(a) and (b) are used to calculate the adsorption rate constants ( $k_1$  and  $k_2$ ) and the amount of adsorption in equilibrium ( $q_e$ ). The calculated kinetics parameters and the correlation coefficient ( $R^2$ ) values

of the two kinetics models are listed in Table 2. As can be observed, the correlation coefficient values of the pseudo-second-order kinetics model are higher than that of the pseudo-first-order kinetics model. Also, the experimental  $q_e$  values are closer to  $q_e$  values calculated from the pseudo-second-order kinetics model. Accordance of the experimental data with the pseudo-second-order kinetics model indicates that the adsorption of MB molecules onto the Harmal seeds residue-based activated carbon is controlled by chemical adsorption [43,44,49–52]. In chemical adsorption, it is assumed that the adsorption capacity is proportional to the number of active sites occupied on the adsorbent surface.

As can be observed in Table 2, the experimental data agree also with the pseudo-first-order kinetic model especially at higher initial concentration of MB,

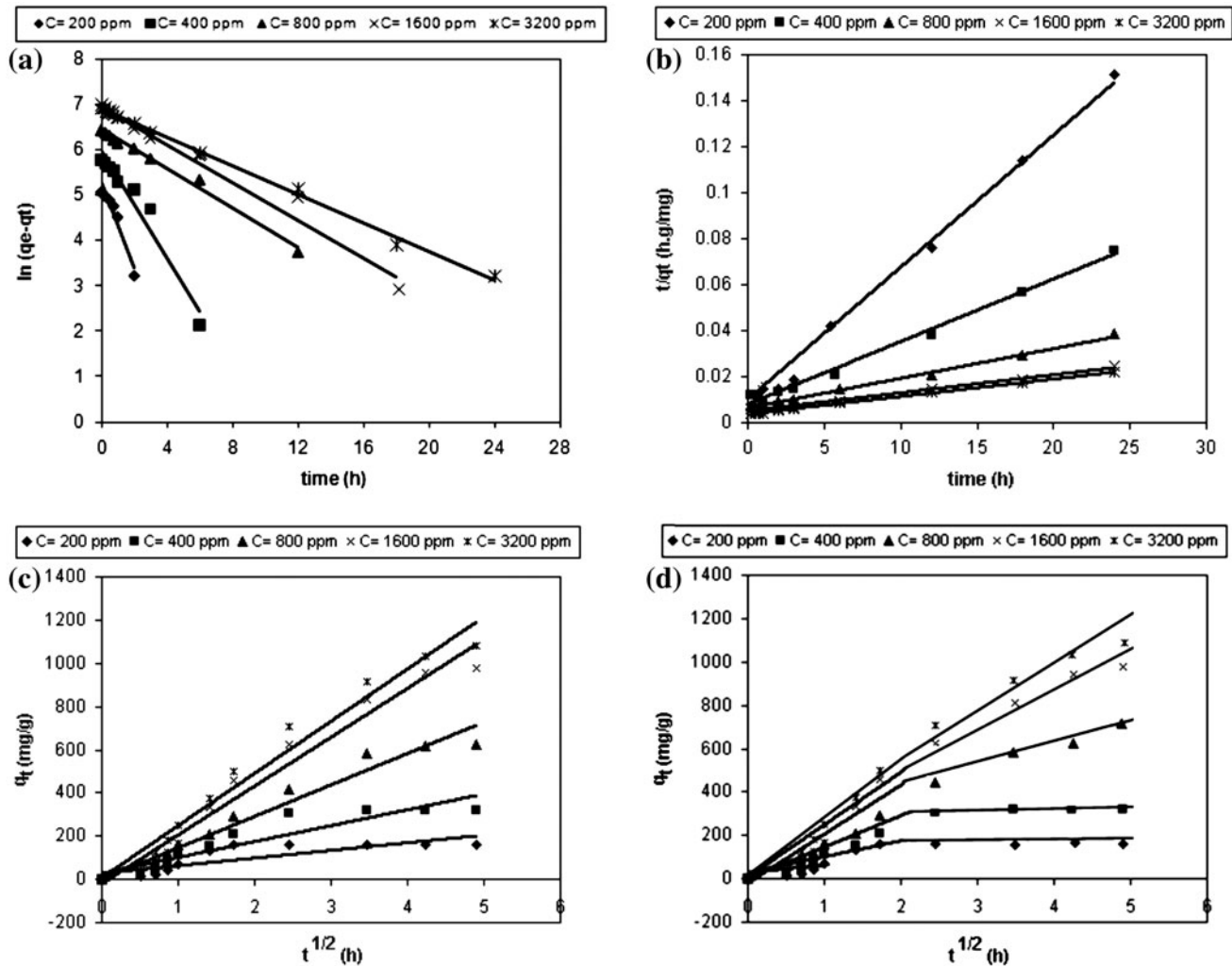


Fig. 9. (a) Pseudo-first-order, (b) Pseudo-second-order, and (c and d) Intraparticle diffusion models for adsorption of MB onto the Harmal seeds residue-based activated carbon.

Table 2

Pseudo-first-order, pseudo-second-order, and intraparticle diffusion models parameters at different initial MB concentrations

Initial MB Cons. (ppm)	$q_{e,exp}$ (mg/g)	Pseudo-first-order kinetic model			Pseudo-second-order kinetic model			Intraparticle diffusion model			
		$q_{e,cal}$ (mg/g)	$k_1$ (h)	$R^2$	$q_{e,cal}$ (mg/g)	$k_2 \cdot 10^{-4}$ (g/g h)	$R^2$	$q_{e,cal}$ (mg/g)	$k_p$ (mg/g h <sup>1/2</sup> )	C	$R^2$
200	158.33	196.40	2.17	0.93	167.74	33.15	0.99	90.43	34.23	31.14	0.67
400	316.66	389.85	1.35	0.94	332.43	9.46	0.99	281.50	73.32	27.52	0.85

(Continued)

which indicates that adsorption of MB onto the Harmal seeds residue-based activated carbon is a diffusion-based process [52,53].

The probability of intraparticle diffusion can be explored by using the intraparticle diffusion model [54]. The intraparticle diffusion model is expressed by:

$$q_t = k_p t^{1/2} + C \quad (9)$$

where  $k_p$  (mg/g h<sup>1/2</sup>) is the intraparticle diffusion rate constant that is obtained from the slope of the straight line of  $q_t$  vs.  $t^{1/2}$  (Fig. 9(c)). The calculated intraparticle diffusion model parameters for MB adsorption onto the Harmal seeds residue-based activated carbon under different initial MB concentrations are listed in Table 2.

As can be observed, the correlation coefficient ( $R^2$ ) values and also the intraparticle diffusion rate constant ( $k_p$ ) values increase with increasing initial MB concentration. This can be explained by the fact that at higher initial concentration, the mass transfer driving force is larger, and hence this results in higher diffusion rates of MB within the pores of adsorbent. In other words, MB adsorption onto the prepared activated carbon takes place probably via chemical adsorption until the surface functional sites are fully occupied; thereafter, MB molecules diffuse into the pores of the adsorbent for further chemical adsorption [1,34,48,55].

The obtained results demonstrate that kinetics of adsorption varies with initial MB concentration. At lower initial MB concentration, adsorption is controlled by chemical adsorption, and to some extent intraparticle diffusion, while at higher initial MB concentration, besides chemical adsorption, intraparticle diffusion is a key mechanism governing the adsorption process [50].

It must be mentioned that plotting  $q_t$  vs.  $t^{1/2}$  provides an indication of the dependency of adsorption

on intraparticle diffusion. If the plot produces a straight line, then the adsorption process is controlled by intraparticle diffusion only. If it exhibits multi-linear plots, then there are two or more steps affecting the adsorption process. It is clear from Fig. 9(d) that the removal of MB by Harmal seeds residue-based activated carbon occurs in two different steps as the plot contains two different straight lines. The first line from 0 to 2 h is attributed to the fast diffusion of the MB molecules from the aqueous phase to the adsorbent surface. The second line from 2 to 5 h is due to the intraparticle diffusion. This confirms that the adsorption of MB by the prepared activated carbon is a multi-step process and involved adsorption to the external surface and diffusion into the pores of the Harmal seeds residue-based activated carbon. The mechanism of MB removal by adsorption is assumed to involve the following steps: (1) migration of MB from the bulk solution to the external surface of adsorbent; (2) diffusion of MB through the boundary layer to the external surface of adsorbent; (3) adsorption of MB at an active site on the surface of adsorbent; and (4) intraparticle diffusion and adsorption of MB through the Harmal seeds residue activated carbon particles [54].

Table 3 presents a comparison of adsorption capacities of MB on a commercial activated carbon and the activated carbon derived from Harmal seeds residue (this work) and other agricultural and industrial wastes. As can be observed, the activated carbon prepared in this work has larger adsorption capacity compared with the others based on the data obtained from the literature. The possibility of formation of dye dimmers, trimmers, etc. and consequently precipitation from the solution due its high initial concentrations (>3,000 ppm) may be partially responsible for high adsorption capacity values, although no precipitation was visually observed.

Table 3

Comparison of the maximum monolayer adsorption capacities of MB on a commercial activated carbon and the activated carbon derived from Harmal seeds residue (this work) and other agricultural and industrial wastes [5]

Adsorbents	Maximum monolayer adsorption capacity (mg/g)
Harmal seeds residue-based activated carbon, (This work)	1111.11
Commercial activated carbon	980.3
Polyvinylidene fluoride activated carbon fibers	486
Straw activated carbon	472.10
Bamboo-based activated carbon	454.20
Activated carbon (molasses/sulfuric acid)	435
Activated carbon prepared from coconut husk	434.78
Vetiver roots activated carbon-H <sub>2</sub> O	423
Peach stones-based activated carbon	412
Oil palm fiber-based activated carbon	400
Mesoporous carbons prepared by using alkaline-treated zeolite	380
Vetiver roots activated carbon-P1.5	375
Rice husk activated carbon	343.50
HCl-treated oil palm shell-based activated carbon	303.03
Rattan sawdust-activated carbon	294.12
Activated carbon prepared from durian shell	289.26
Coconut shell activated carbon	277.90
Oil palm fiber-based activated carbon	277.78
Olive-seed waste residue-based activated carbon	190–263
Activated carbon prepared from oil palm shell	243.90
<i>Hevea brasiliensis</i> seed coat- activated carbon	227.27
Activated tyre char	227
Jute fiber carbon	225.64
Mesoporous carbon prepared by using acid-treated zeolite	223
Activated furniture (850 °C)	200
Dehydrated wheat bran carbon	185.2
Groundnut sell activated carbon	164.90
Bamboo dust activated carbon	143.20
Activated tyre (850 °C)	130
Chemically activated <i>Salsola vermiculata</i> plant	130
Activated sewage char (800 °C)	120
Activated carbon prepared from a renewable bio-plant of <i>Euphorbia rigida</i>	109.98
Waste apricot-based activated carbon	102

#### 4. Conclusion

Harmal seeds residue-based activated carbon was prepared and used as a practical adsorbent for MB removal from aqueous solutions. The results demonstrated that adsorption capacity of prepared activated carbon increases with increasing initial MB concentration. Adsorption behavior of MB molecules onto the prepared activated carbon match well with Langmuir isotherm model with maximum monolayer adsorption capacity of 1111.11 mg/g. Adsorption kinetics follows the pseudo-second-order kinetic model. At higher initial MB concentrations, besides chemical adsorption, intraparticle diffusion is a key mechanism governing

the adsorption process. Following the above results, the Harmal seeds residue-based activated carbon can be recommended as an effective adsorbent for MB removal from wastewater.

#### References

- [1] M. Banat, P. Nigam, D. Singh, R. Marchant, Microbial decolorization of textile-dye-containing effluents: A review, *Bioresour. Technol.* 58 (1996) 217–227.
- [2] T. Robinson, G. McMullan, R. Marchant, P. Nigam, Remediation of dyes in textile effluent: A critical review on current treatment technologies with a proposed alternative, *Bioresour. Technol.* 77 (2001) 247–255.
- [3] G. Crini, Non-conventional low cost adsorbents for dye removal: A review, *Bioresour. Technol.* 97 (2006) 1061–1085.

- [4] B.H. Hameed, A.L. Ahmad, K.N.A. Latiff, Adsorption of basic dye (methylene blue) onto activated carbon prepared from rattan sawdust, *Dyes Pigm.* 75 (2007) 143–149.
- [5] M. Rafatullah, O. Sulaiman, R. Hashim, A. Ahmad, Adsorption of methylene blue on low-cost adsorbents: A review, *J. Hazard. Mater.* 177 (2010) 70–80.
- [6] I.A.W. Tan, B.H. Hameed, A.L. Ahmad, Equilibrium and kinetic studies on basic dye adsorption by oil palm fiber activated carbon, *Chem. Eng. J.* 127 (2007) 111–119.
- [7] A.K. Jain, V.K. Gupta, A. Bhatnagar, Suhas Utilization of industrial waste products as adsorbents for the removal of dyes, *J. Hazard. Mater. B* 101 (2003) 31–42.
- [8] F. Derbyshire, M. Jagtoyen, R. Andrews, A. Rao, I. Martin-Gullon, E. Grulke, Carbon materials in environmental applications, in: L.R. Radovic (Ed.), *Chemistry and Physics of Carbon*, vol. 27, Marcel Dekker, New York, NY, 2001, pp. 1–66.
- [9] X.S. Wang, H.Q. Lin, Adsorption of basic dyes by dried waste sludge: Kinetic, equilibrium and desorption studies, *Desalin. Water Treat.* 29 (2011) 10–19.
- [10] A.A. Attia, B.S. Girgis, N.A. Fathy, Removal of methylene blue by carbons derived from peach stones by  $H_3PO_4$  activation: Batch and column studies, *Dyes Pigm.* 76 (2008) 282–289.
- [11] M.J. Martin, A. Artola, M.D. Balaguer, M. Rigola, Activated carbons developed from surplus sewage sludge for the removal of dyes from dilute aqueous solutions, *Chem. Eng. J.* 94 (2003) 231–239.
- [12] M.M.A. El-Latif, A.M. Ibrahim, Removal of reactive dye from aqueous solutions by adsorption onto activated carbons prepared from oak sawdust, *Desalin. Water Treat.* 20 (2010) 102–113.
- [13] K.Y. Foo, Bassim H. Hameed, An overview of dye removal via activated carbon adsorption process, *Desalin. Water Treat.* 19 (2010) 255–274.
- [14] N. Bouchemal, F. Addoun, Adsorption of dyes from aqueous solution onto activated carbons prepared from date pits: The effect of adsorbents pore size distribution, *Desalin. Water Treat.* 7 (2009) 242–250.
- [15] M. Belhachemi, Z. Belala, D. Lahcene, F. Addoun, Adsorption of phenol and dye from aqueous solution using chemically modified date pits activated carbons, *Desalin. Water Treat.* 7 (2009) 182–190.
- [16] M. Benadjemia, L. Millière, L. Reinert, N. Benderdouche, L. Duclaux, Preparation, characterization and methylene blue adsorption of phosphoric acid activated carbons from globe artichoke leaves, *Fuel Process. Technol.* 92 (2011) 1203–1212.
- [17] N. Tancredi, N. Medero, F. Möller, P. Javier, P. Carina, T. Cordero, Phenol adsorption onto powdered and granular activated carbon, prepared from eucalyptus wood, *J. Colloid Interface Sci.* 279 (2004) 357–363.
- [18] K.M. Smith, G.D. Fowler, S. Pullket, N.J.D. Graham, The production of attrition resistant, sewage-sludge derived, granular activated carbon, *Sep. Purif. Technol.* 98 (2012) 240–248.
- [19] R.R. Bansode, J.N. Lasso, W.E. Marshall, R.M. Rao, R.J. Portier, Adsorption of metal ions by pecan shell-based granular activated carbons, *Bioresour. Technol.* 89 (2003) 115–119.
- [20] H.R. Monsef, A. Ghobadi, M. Iranshahi, M. Abdollahi, Antinociceptive effects of *Peganum harmala* L. alkaloid extract on mouse formalin test, *J. Pharm. Pharm. Sci.* 7 (1) (2004) 65–69.
- [21] [www.wikipedia.org/wiki/Harmal](http://www.wikipedia.org/wiki/Harmal).
- [22] D. Prashanth, S. John, Antibacterial activity of *Peganum harmala*, *Fitoterapia* 70(4) (1999) 438–439.
- [23] N. Arshad, K. Zitterl-Eglseder, S. Hasnain, M. Hess, Effect of *Peganum harmala* or its beta-carboline alkaloids on certain antibiotic resistant strains of bacteria and protozoa from poultry, *Phytother. Res.* 22(11) (2008) 1533–1538.
- [24] R. Jbilou, H. Amri, N. Bouayad, N. Ghailani, A. Ennabili, F. Sayah, Insecticidal effects of extracts of seven plant species on larval development, alpha-amylase activity and offspring production of *Tribolium castaneum* (Herbst) (Insecta: Coleoptera: Tenebrionidae), *Bioresour. Technol.* 99(5) (2008) 959–964.
- [25] Q. El-Dwairi, S. Banihani, Histo-functional effects of *Peganum harmala* on male rat's spermatogenesis and fertility, *Neuro. Endocrinol. Lett.* 28(3) (2007) 305–310.
- [26] C. Bouchelta, M.S. Medjram, O. Bertrand, J.-P. Bellat, Preparation and characterization of activated carbon from date stones by physical activation with steam, *J. Anal. Appl. Pyrolysis* 82 (2008) 70–77.
- [27] Q.A. Ioannidou, A.A. Zabaniotou, G.G. Stavropoulos, Md.A. Islam, T.A. Albanis, Preparation of activated carbons from agricultural residues for pesticide adsorption, *Chemosphere* 80 (2010) 1328–1336.
- [28] Yong Sun, Paul A. Webley, Preparation of activated carbons from corncob with large specific surface area by a variety of chemical activators and their application in gas storage, *Chem. Eng. J.* 162 (2010) 883–892.
- [29] S.B. Wang, G.Q. Lu, Effects of acidic treatments on the pore and surface properties of Ni catalyst supported on activated carbon, *Carbon* 36 (1998) 283–292.
- [30] S. Wang, Z.H. Zhu, A. Coomes, F. Haghsereht, G.Q. Lu, The physical and surface chemical characteristics of activated carbons and the adsorption of methylene blue from wastewater, *J. Colloid Interface Sci.* 284 (2005) 440–446.
- [31] D. Xu, X.L. Tan, C.L. Chen, X.K. Wang, Removal of Pb (II) from aqueous solution by oxidized multi-walled carbon nanotubes, *J. Hazard. Mater.* 154 (2008) 407–417.
- [32] S.M. Chen, W.M. Shen, G.Z. Wu, D.Y. Chen, M. Jiang, A new approach to the functionalization of single-walled carbon nanotubes with both alkyl and carboxyl groups, *Chem. Phys. Lett.* 402 (2005) 312–317.
- [33] Y.H. Yan, J. Cui, M.B. Chan-Park, X. Wang, Q.Y. Wu, Systematic studies of covalent functionalization of carbon nanotubes via argon plasma-assisted UV grafting, *Nanotechnology* 18 (2007) 115712 (1–7).
- [34] J. Wang, X. Ma, G. Fang, M. Pan, X. Ye, S. Wang, 353 Preparation of iminodiacetic acid functionalized multi-walled carbon nanotubes and its application as sorbent for separation and preconcentration of heavy metal ions, *J. Hazard. Mater.* 186 (2011) 1985–1992.
- [35] G.D. Vuković, A.D. Marinković, M. Čolić, M.D. Ristić, R. Aleksić, A.A. Perić-Grujić, P.S. Uskoković, Removal of cadmium from aqueous solutions by oxidized and ethylenediamine-functionalized multi-walled carbon nanotubes, *Chem. Eng. J.* 157 (2010) 238–248.
- [36] M.A. Tofighy, T. Mohammadi, Application of Taguchi experimental design in optimization of salty water desalination using purified carbon nanotubes as adsorbent, *Mater. Res. Bull.* 47 (2012) 2389–2395.
- [37] A. Stafiej, K. Pyrzynska, Adsorption of heavy metal ions with carbon nanotubes, *Sep. Purif. Technol.* 58 (2008) 49–52.
- [38] K. Pyrzynska, Application of carbon sorbents for the concentration and separation of metal ions, *Anal. Sci.* 23 (2007) 631–637.
- [39] M.A. Tofighy, T. Mohammadi, Salty water desalination using carbon nanotube sheets, *Desalination* 258 (2010) 182–186.
- [40] F. Su, Ch. Lu, S. Hu, Adsorption of benzene, toluene, ethylbenzene and p-xylene by NaOCl-oxidized carbon nanotubes, *Colloids Surf. A Physicochem. Eng. Asp.* 353 (2010) 83–91.
- [41] X. Ren, Ch. Chen, M. Nagatsu, X. Wang, Carbon nanotubes as adsorbents in environmental pollution management: A review, *Chem. Eng. J.* 170 (2011) 395–410.
- [42] Sh. Yang, J. Li, D. Shao, J. Hu, X. Wang, Adsorption of Ni (II) on oxidized multi-walled carbon nanotubes: Effect of contact time, pH, foreign ions and PAA, *J. Hazard. Mater.* 166 (2009) 109–116.
- [43] A. Özer, G. Dursun, Removal of methylene blue from aqueous solution by dehydrated wheat bran carbon, *J. Hazard. Mater.* 146 (2007) 262–269.
- [44] I.A.W. Tan, A.L. Ahmad, B.H. Hameed, Adsorption of basic dye on high-surface-area activated carbon prepared from coconut husk: Equilibrium, kinetic and thermodynamic studies, *J. Hazard. Mater.* 154 (2008) 337–346.

- [45] T.W. Weber, R.K. Chakkravorti, Pore and solid diffusion models for fixed bed adsorbers, *AIChE J.* 20 (1974) 228–238.
- [46] B. Bestani, N. Benderdouche, B. Benstaali, M. Belhakem, A. Addou, Methylene blue and iodine adsorption onto activated desert plant, *Bioresour. Technol.* 99 (2008) 8441–8444.
- [47] S. Lagergren, B.K. Svenska, Zur theorie der sogenannten adsorption gelöster stoffe, *Veternskapsakad Handlingar* 24(4) (1898) 1–39.
- [48] Y.S. Ho, G. McKay, Sorption of dye from aqueous solution by peat, *Chem. Eng. J.* 70 (1998) 115–124.
- [49] W. Zou, R. Han, Z. Chen, Z. Jinghua, J. Shi, Kinetic study of adsorption of Cu(II) and Pb(II) from aqueous solutions using manganese oxide zeolite in batch mode, *Colloids Surf. A Physicochem. Eng. Asp.* 279 (2006) 238–246.
- [50] M.A. Tofighy, T. Mohammadi, Permanent hard water softening using carbon nanotube sheets, *Desalination* 268 (2011) 208–213.
- [51] Y.S. Ho, G. McKay, Pseudo-second order model for sorption processes, *Process Biochem.* 34 (1999) 451–465.
- [52] M.A. Tofighy, T. Mohammadi, Adsorption of divalent heavy metal ions from water using carbon nanotube sheets, *J. Hazard. Mater.* 185 (2011) 140–147.
- [53] M. Hamdi, M. Dogan, M. Alkan, Kinetic analysis of reactive blue 221 adsorption on kaolinite, *Desalination* 256 (2010) 154–165.
- [54] H. Al-Johani, M. Abdel Salam, Kinetics and thermodynamic study of aniline adsorption by multi-walled carbon nanotubes from aqueous solution, *J. Colloid Interface Sci.* 360 (2011) 760–767.
- [55] Y. Yao, B. He, F. Xu, X. Chen, Equilibrium and kinetic studies of methyl orange adsorption on multiwalled carbon nanotubes, *Chem. Eng. J.* 170 (2011) 82–89.